

# Generation of Chaos using Ramanujans Ternary Quadratic Form

Sai Venkatesh Balasubramanian

*Sree Sai Vidhya Mandhir, Mallasandra, Bengaluru-560109, Karnataka, India.  
saivenkateshbalasubramanian@gmail.com*

---

## Abstract

Ramanujans Ternary Quadratic Form represents a series of numbers that satisfy a tripartite quadratic relation. In the present work, we examine the sequence of numbers generated by such forms and other related forms obtained by varying the coefficients and exponents to other values. Chaotic characterization using standard techniques such as Lyapunov Exponents, Kolmogorov Entropy, Fractal Dimensions, Phase Portraits and Distance plots is performed. It is seen that the Ramanujans Form as well as the related forms, when expressed as time series exhibit chaotic behavior. Finally, we conclude by stating that the form to series mapping outlined in the present work enables the generation of chaotic signals without the need for excessive system complexity and memory, and we note that such chaotic signals can be used as the basis for carriers in secure communication systems.

*Keywords:* Ramanujans Ternary Quadratic Form, Chaos Generation, Chaotic Characterization

---

## 1. Introduction

As the flagship of Nonlinear Science, Chaos Theory has found applications in diverse fields such as astronomy, biology, physics and engineering [1, 2, 3]. It has broadened mans perspective of nature by successfully modeling and representing the pattern formation of many natural phenomena [4, 5, 6]. From a mathematical perspective, the ability of complex and ornate behavior arising out of simple system nonlinearities form the piece de resistance of chaos theory [4, 5, 6].

In real time technology, chaos generation has been successfully applied in secure communication and encryption systems [7, 8]. The Sensitive Dependence to Initial Conditions, one of the key signatures of chaos is seen to ensure a high degree of security in such systems [1, 2, 6].

The traditional method of generating chaotic signals has been using partial differential equations to model a chaotic system, and by studying the behavior of such systems using iterative maps and bifurcation diagrams, appropriate values for control parameters are set, and as a consequence, chaos is generated [1, 2, 6]. The generated chaotic signal is then characterized using standard parameters such as Kolmogorov Entropy, Fractal Dimension and Lyapunov Exponent, which give an indication to the nature of chaos generated [9, 10, 11].

However, the present work takes a radically different approach to generating chaos. We start with a number theory basis, where a mathematical form such as Ramanujans Ternary Quadratic Form is defined [12, 13, 14]. By considering the algebraic variables of the form as the coordinates and iterating the form for increasing values of each coordinate, we obtain a time series. We then use the standard characterization techniques to ascertain the chaotic nature of the generated time series. The characterization results indeed reveal chaotic behavior of the generated time series. It is noted that the iteration can be performed in any standard hardware system such as a Microcontroller or FPGA without consuming too much memory or increasing system complexity. This simplicity of the proposed chaos generation, coupled with the characterized parameters form the major results of the work.

## 2. Deriving the Time Series from Ramanujan Ternary Quadratic Form

The basis of the chaos generation proposed in the present work is a mathematical form defined in number theory. Specifically, Ramanujans Ternary Quadratic Form (RTQF) is chosen cite12. RTQF was formulated initially by Ramanujan to form the necessary and sufficient conditions for the inability to represent an integer in the algebraic form  $Ax^2 + By^2 + Cz^2$  for certain specific values of A, B and C [12, 13, 14].

The Ramanujan Ternary Quadratic Form is given by the following algebraic expression:

$$S = x^2 + y^2 + 10z^2 \tag{1}$$

where x, y and z are algebraic variables, and A=1; B=1; C=10 are the coefficients. In the present work, x, y and z are visualized as the coordinates of a 3 dimensional system.

By an iterative procedure, it is possible to map the three coordinates into a single coordinate representing time, thus effectively rendering S as a time series, whose limits are defined by the limits of the iterations. For instance, if x, y and z are iterated M, N and P times respectively, then S is a time series consisting of MxNxP samples. The iteration/mapping process can be concisely explained by the following pseudocode:

```

For i in 1 to M;
For j in 1 to N;
For k in 1 to P;
 $S = i^2 + j^2 + 10^2;$ 
End k; End j; End i;

```

In the present work, the values of M, N and P are set as 15 and thus the time series S consists of 3375 samples.

In addition to the original RTQF form described in Equation 1, a variety of other forms obtained by varying the coefficients A, B and C are explored for chaos generation. The present paper elaborates on three such RTQF deviations, as listed below. For each of the cases, the form generated is mapped into a time series as given by the above iterative procedure.

In order to observe any variations caused due to higher exponents of x, y and z, two variants of the RTQF as well as each of the three deviations described below are considered. For each case, the first variant is quadratic, with the powers of x, y and z set as 2. The second is a cubic variant, using the third power of x, y and z. In the case of RTQF, these variants are denoted as RTQF-2 and RTQF-3 respectively. Thus Equation 1 is a representation of RTQF-2. RTQF-3 is given as follows:

$$S = x^3 + y^3 + 10z^3 \quad (2)$$

### 2.1. The Phi-Pi Form

This form is obtained by setting the values of A, B and C as A=1, B= $\phi$  and C= $\pi$ , where  $\phi$  ('Phi') represents the mathematical golden ratio 1.61803 and  $\pi$  ('Pi') represents the mathematical constant relating the circumference and diameter of a circle and given by 3.141592. The Phi-Pi-2 and Phi-Pi-3 forms are given as follows.

$$S = x^2 + \phi y^2 + \pi z^2; S = x^3 + \phi y^3 + \pi z^3 \quad (3)$$

### 2.2. The Pythagorean Form

Here, A=3; B=4 and C=5. The basis of this form is the fact that the values of 3, 4 and 5 satisfy the Pythagorean relation  $a^2 + b^2 = c^2$  representing the sides of a right angled triangle. Thus the Pythagorean-2 and Pythagorean-3 forms are as follows.

$$S = 3x^2 + 4y^2 + 5z^2; S = 3x^3 + 4y^3 + 5z^3 \quad (4)$$

### 2.3. The OEN Form

The coefficient values here are set as A=1, B=8 and C=9. The motivation for using this combination of coefficients is that the numerological values (digit sums) of the cubes 1,8,27,64,125,216,343, of the natural numbers 1,2,3,4,5,6,7, result in a regular periodic pattern of 1,8,9,1,8,9,1,. It is noteworthy that such a repeating periodic sequence is not seen in the digit sums of squares, and the name OEN is derived from the three numbers present in the sequence One(O), Eight(E) and Nine(N). The OEN-2 and OEN-3 forms are then given as follows:

$$S = x^2 + 8y^2 + 9z^2; S = x^3 + 8y^3 + 9z^3 \quad (5)$$

The Equations 1 to 5, coupled with the iteration procedure mentioned earlier give rise to time series, whose characterization shall now be discussed.

## 3. Chaotic Characterization of the Time Series

In order to ascertain the nature of chaos generated by mapping the Ramanujans Ternary Quadratic and related Forms as elaborated above, the characterization of time series using nonlinear analysis principles is preformed. The Characterization techniques are grouped into Qualitative, consisting of Time Series, Phase Portrait and Distance Map, and Quantitative consisting of Kolmogorov Entropy, Lyapunov Exponents and Fractal Dimension. The results of the qualitative analyses of the -2 and -3 versions of each of the 4 cases of RTQF, Phi-Pi, Pythagorean and OEN and illustrated in Fig. 1 to Fig. 8.

### 3.1. Time Series

The time series is obtained by mapping the three coordinates  $x, y$  and  $z$  into a single time coordinate as per the iterative procedure described in Snippet 1. From the time series shown in Fig. 1 to Fig. 8, we see that in all the cases, the time series consists of a tandem of exponentially increasing envelopes with abrupt breaks in between. The degree of curvature of the time series is governed by the value of coefficients.

### 3.2. Phase Portrait

One of the significant analysis techniques for a chaotic signal is to plot its phase portrait [1, 2, 3]. This portrait, depicting the time derivative of a signal ( $dS/dt$ ) as a function of the signal ( $S$ ) illustrates the dynamics of the signal in the phase space [3, 4, 6]. This describes the stability aspects of the chaotic system behavior and points of stability around which the system revolves, qualitatively serving as a tool to assess various chaotic parameters such as sensitivity and ergodicity [1, 2, 3, 4, 5, 6]. The phase portraits of the various cases shown in Fig. 1 to Fig. 8 highlight the following key points:

1. The RTQF-2 and RTQF-3 phase portraits resemble a triangular pattern, showing little variation in the triangle edge lengths. RTQF-3 phase portrait shows a slightly wider spacing between the vertical edges of the triangle.
2. Phi-Pi-2 and Phi-Pi-3 phase portraits consist of an outer triangle and an inner triangle, with the latter showing considerably higher ergodicity. Here too, the inner triangle edge spacings in the Phi-Pi-3 case are clearer.
3. Similar to the Phi-Pi-2 and Phi-Pi-3 cases, the Pythagorean-2 and Pythagorean-3 case phase portraits consist of an outer triangle and a more ergodic inner triangle. The key factor differentiating the Phi-Pi and Pythagorean patterns is the higher amount of horizontal drag observed in the latter.
4. The OEN-2 and OEN-3 phase portraits extend the formation of inner triangle and horizontal offset one step further the OEN phase portraits, particularly OEN-3 describe a remarkable regularity in the spacing of the inner triangles. On observing the spacing from right to left, one observes a monotonic decrease in spacing, reminiscent of a logarithmic axis.
5. In all the phase portraits, the signal and derivative amplitude ranges for the -3 case are higher than the -2 case.

### 3.3. Distance Maps

The Distance Map for a time series  $S$  with  $R$  samples is the graphical representation of the Distance Matrix, a two dimensional  $R \times R$  matrix, where any point  $(i, j)$  denotes the distance between the  $i$ th and  $j$ th sample of  $S$  [15, 16]. Thus, for pairs of points lying fairly close to each other in the amplitude space, the distance matrix yields a low value. The distance map and its derivative, the recurrence map, have been used to characterize the recurrences of states, since the arbitrary closeness of values after a certain time of divergence is a significant characteristic of deterministic dynamical systems including Chaos [15, 16]. The following points can be observed from the Distance Maps of Fig. 1 to Fig. 8. The maps are plotted using the jet color map, with the intensity increasing from blue to red.

1. The distance maps of RTQF-2 and RTQF-3 depict a dense collection of repeating elements with significantly low amplitude variations, suggesting a tendency towards periodicity.
2. Phi-Pi-2 and Phi-Pi-3 distance maps show a collection of repeating elements with a larger variation in the intensities, with the contrast of Phi-Pi-3 higher than Phi-Pi-2.
3. The Pythagorean distance maps improve the contrast even further, and the larger set of repeating elements is observed here too.
4. The OEN distance maps show the highest contrasts of the four forms. However, the pattern of repeating elements is observed here too.

### 3.4. Lyapunov Exponent

The chaotic nature of the generated signal is assertively established by calculating the largest Lyapunov Exponent (LLE), a measure of a systems sensitive dependence on initial conditions [9]. Rosensteins algorithm is used to compute the Lyapunov Exponents  $\lambda_i$  from the time series, where the sensitive dependence is characterized by the divergence samples  $d_j(i)$  between nearest trajectories represented by  $j$  given as follows,  $C_j$  being a normalization constant [9, 10]:

$$d_j(i) = C_j e^{\lambda_i(i\delta t)} \quad (6)$$

The LLE values obtained for the 4 cases with -2 and -3 variants are tabulated in Table 1. The following are inferred:

1. In the Phi-Pi and the Pythagorean cases, the LLEs for the -2 variants are greater than the -3 counterparts, whereas in the OEN and RTQF cases, this trend is reversed.

Table 1: Quantitative Chaotic Characterization of the four mathematical forms

Basic Form	$K$ (bits/sym)	$D$	$LLE$
RTQF-2	7.8552	0.9037	2.3514
RTQF-3	7.7144	0.9037	2.9020
Phi-Pi-2	7.9667	0.9037	2.8060
Phi-Pi-3	7.8731	0.9037	2.6972
Pythagorean-2	7.9880	0.9037	2.5289
Pythagorean-3	7.9037	0.9037	2.3989
OEN-2	7.9467	0.9037	2.3169
OEN-3	7.8413	0.9037	3.1357

- Among the -2 variants, the OEN-2 shows the lowest LLE whereas for the -3 variants, the OEN-3 LLE is the highest. This might intuitively suggest the use of the OEN mathematical form being more suitable to the third order, since the basis for deriving the OEN numbers were from the third order.
- Among the -2 variants, Phi-Pi-2 shows highest LLE, intuitively suggesting the ubiquity of the universal mathematical constants of  $\phi$  and  $\pi$ .

### 3.5. Kolmogorov Entropy

The worthiness of the generated signal as a potential telecommunication carrier can be established by ascertaining the amount of information that can be carried by the signal. This is precisely quantified by the Kolmogorov Entropy, a statistical measure of the uncertainty of the signal [9]. By assigning each of the  $R$  quantifiable states of the amplitude of the output signal as an event  $i$ , the Kolmogorov Entropy  $K$  obtained depends on their probabilities  $p_i$  according to the relation as follows:

$$K = - \sum_{i=1}^N p_i \log p_i \quad (7)$$

- For all the 4 cases as seen from Table 1,  $K$  is higher in the -2 variants than the -3 variants.
- The absolute highest value of  $K$  is obtained for the Pythagorean-2 case, whereas RTQF-3 exhibits the lowest entropy.
- There is no definite correlation discernable between the obtained values of  $K$  and  $LLE$ .

### 3.6. Fractal Dimension

The chaotic/fractal nature of the signal is further confirmed by computing the fractal dimension, using the Minkowski Bouligand Box Counting Method [11]. In this method, various square boxes of different sizes  $e$  are formed and for each size  $e$ , the number of boxes  $N(e)$  required to cover the entire set is computed. The fractal dimension  $D$  is then given as follows [11]

$$D = \lim_{e \rightarrow 0} \frac{\log(N(e))}{\log(e)} \quad (8)$$

From Table 1, it is observed that for all the 4 cases with the -2 and -3 variants, the Fractal Dimension remains unchanged at 0.9037, the non-integral value asserting chaotic presence.

## 4. Conclusion

A radically different approach to generation of chaos using a number theory basis is proposed. Ramanujans Ternary Quadratic Form (RTQF) is chosen as the basis and, by using an iterative procedure, the three coordinates of the form are mapped onto a 1D time series. Three deviations from the RTQF by way of different coefficients and exponents are explored, and for each of the four cases (RTQF plus 3 deviations), the generated time series is characterized qualitatively using time series, phase portrait and distance maps, and quantitatively using Lyapunov Exponents, Kolmogorov Entropy and Fractal Dimension. The Characterization Results attest to the presence of chaotic behavior in all the generated time series, with the highest sensitivity obtained for the OEN-3 case.

Thus, the mapping of various mathematical forms into time series forms the base algorithm for the generation of chaos, and this algorithm can be implemented on a software level or on a hardware level using platforms such as Microcontrollers and FPGAs. It is noteworthy that the implementations can be carried out with minimal computing requirements since,

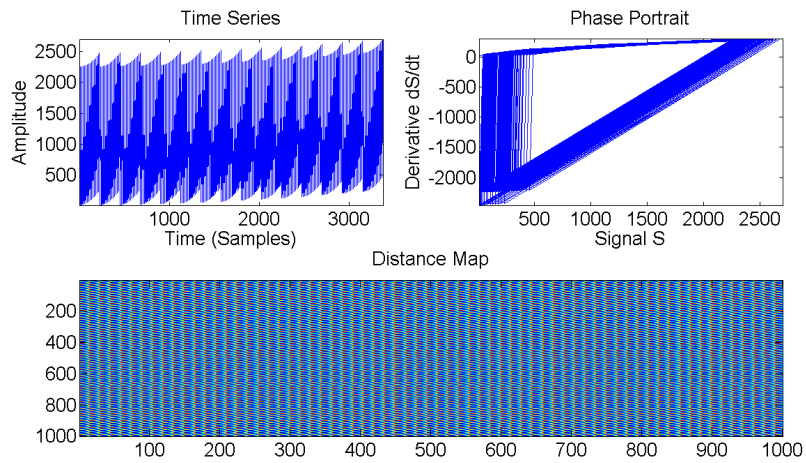


Figure 1: Qualitative Characterization of Chaos generated using RTQF-2 Form

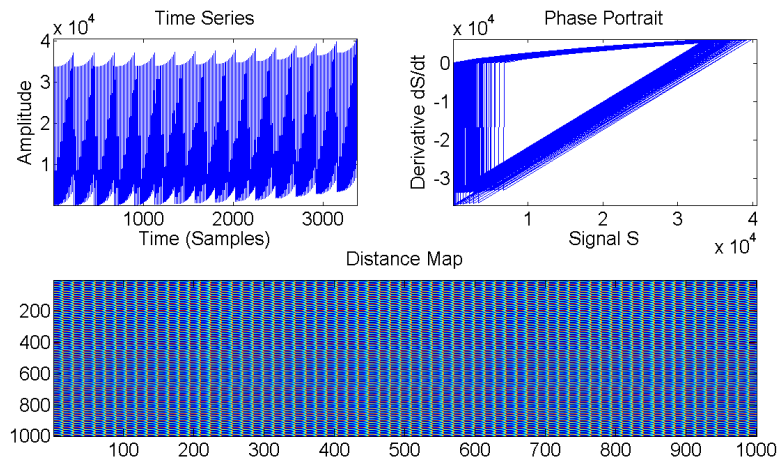


Figure 2: Qualitative Characterization of Chaos generated using RTQF-3 Form

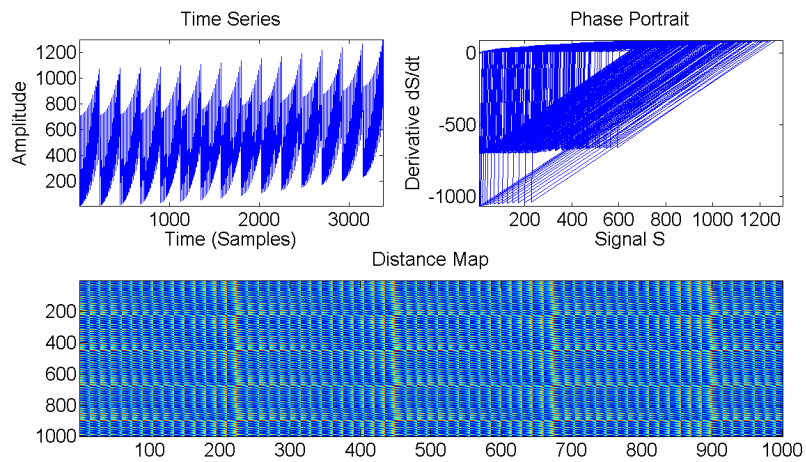


Figure 3: Qualitative Characterization of Chaos generated using Phi-Pi-2 Form

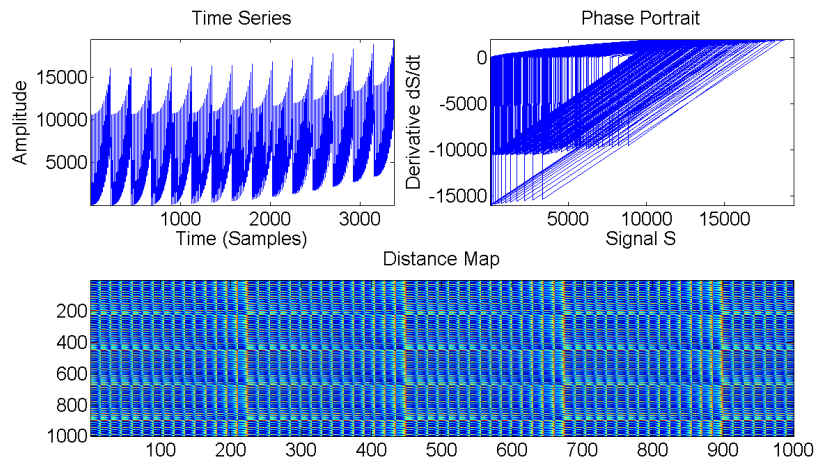


Figure 4: Qualitative Characterization of Chaos generated using Phi-Pi-3 Form

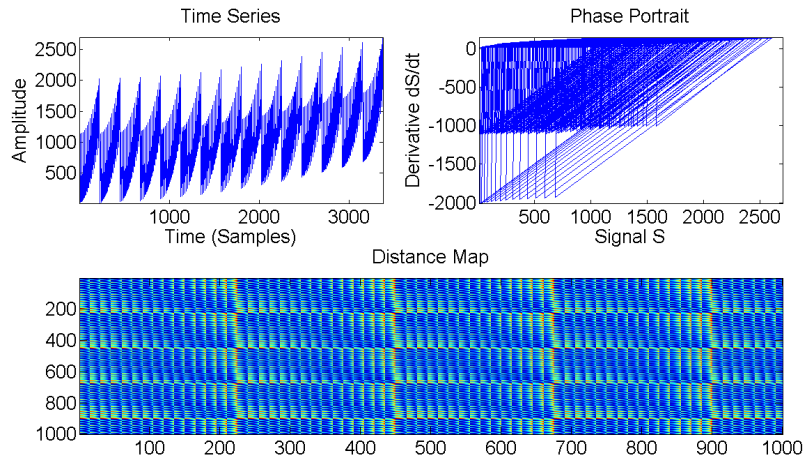


Figure 5: Qualitative Characterization of Chaos generated using Pythagorean-2 Form

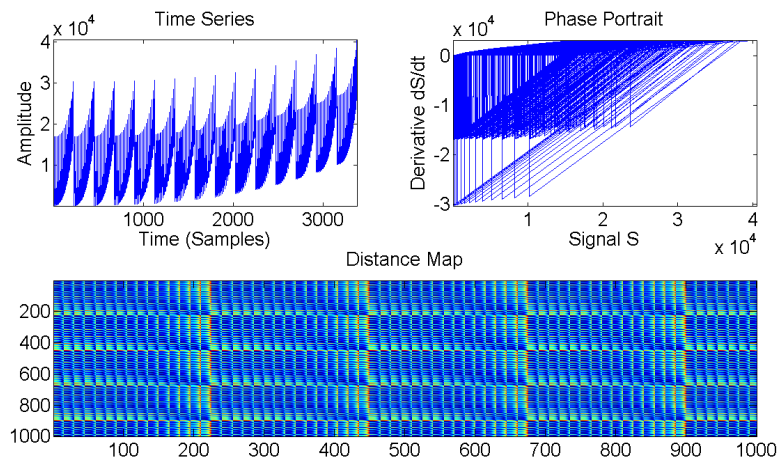


Figure 6: Qualitative Characterization of Chaos generated using Pythagorean-3 Form

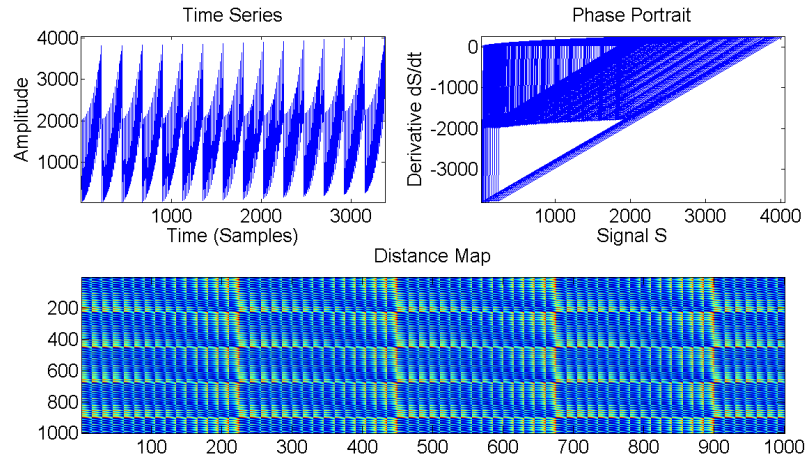


Figure 7: Qualitative Characterization of Chaos generated using OEN-2 Form

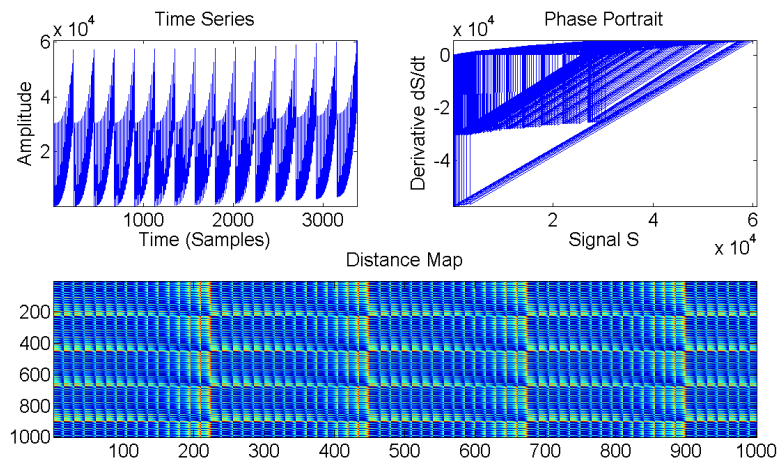


Figure 8: Qualitative Characterization of Chaos generated using OEN-3 Form

unlike conventional iterative maps, there is no dependence on the previous iteration values, making it in principle a memoryless implementation. The simplicity of the proposed chaos generation, coupled with the characterized results confirming chaotic nature, and the direct applicability of the generated chaos in secure communication applications forms the novelty of the present work.

## References

- [1] M. Ausloos, M. Dirickx, *The Logistic Map and the Route to Chaos: From the Beginnings to Modern Applications*, (Springer, US, [2006]).
- [2] S. H. Strogatz, *Nonlinear Dynamics and Chaos: With Applications to Physics, Biology, Chemistry, and Engineering*, (Westview Press, Cambridge, 2008).
- [3] M. H. Jensen, P. Bak, T. Bohr, Complete Devils Staircase, Fractal Dimension, and Universality of Mode-Locking Structure in the Circle Map, *Phys. Rev. Lett.* 50, 1637 (1983).
- [4] G. B. Giannakis, F. Bach, R. Cendrillon, M. Mahoney, J. Neville, Signal Processing for Big Data, *IEEE Signal Processing Magazine*, 31, 15-16 (2014).
- [5] M. Hilbert, How much of the global information and communication explosion is driven by more, and how much by better technology?, *Wiley Journal of the Association for Information Science and Technology*, 65, 856-861 (2014).
- [6] E. Bilotta and P. Pantano, *A gallery of Chua attractors*, (World Scientific, Singapore, 2008).
- [7] M. F. Barnsley, A. D. Sloan, *Chaotic Compression*, *Computer Graphics World*, 3 (1987).
- [8] K. E. Barner and G. R. Arce, *Nonlinear Signal and Image Processing: Theory, Methods, and Applications*, (CRC Press, U.S, 2003).
- [9] R. G. James, K. Burke, J. P. Crutchfield, Chaos forgets and remembers: Measuring information creation, destruction, and storage, *Int. J. Bifurcation Chaos*. 378, 2124 (2014).
- [10] M. T. Rosenstein, J. J. Collins, C. J. De Luca, A practical method for calculating largest Lyapunov exponents from small data sets, *Physica D*, 65, 117, (1993).
- [11] P. Maragos, F. K. Sun, Measuring the fractal dimension of signals: morphological covers and iterative optimization, *IEEE Trans. Signal Processing*, 41, 108-121 (1993).
- [12] K. Ono, K. Soundararajan, Ramanujan's ternary quadratic form, *Inventiones Mathematicae*, 130, 415-454 (1993).
- [13] B. W. Jones, G. Pall, Regular and semi-regular positive ternary quadratic forms, *Acta Mathematica* 70, 165-191 (1939).
- [14] H. Gupta, Some idiosyncratic numbers of Ramanujan, *Proceedings of the Indian Academy of Sciences Section A*, 13, 519-520 (1941).
- [15] J. P. Eckmann, S. O. Kamphorst, D. Ruelle, Recurrence Plots of Dynamical Systems, *Europhysics Letters* 5, 973-977 (1987).
- [16] N. Marwan, M. C. Romano, M. Thiel, J. Kurths, Recurrence Plots for the Analysis of Complex Systems, *Physics Reports* 438, 237 (2007).